

ScholarWorks@GSU

Synthesis of Near-infrared Heptamethine Cyanine Dyes as Biological Imaging Agents

Authors	Malray, Jordan L
Download date	2026-05-13 16:26:14
Link to Item	https://hdl.handle.net/20.500.14694/7449

Synthesis of a Heptamethine and Trimethine Cyanine Dye as a Biological Imaging Agent

Jordan L. Malray

Georgia State University, Department of Chemistry

I. Abstract

For this experiment, a near-infrared (NIR) heptamethine cyanine dye was synthesized using a multi-step synthetic approach. Normal biological tissues absorb light in the visible region of the electromagnetic spectrum, whereas (NIR) polymethine cyanine dyes exhibit longer wavelengths that cannot be detected by the naked eye. Using FLARE imaging technology, both visible and NIR light can now be distinguished simultaneously, with both images superimposed to create a more detailed picture of a specific target. Using this technique, surgeons were able to determine the heptamethine dye's binding habits in CD-1 mice, which showed uptake in the vasculature of the brain.

II. Introduction

The known history of cyanine dyes began in 1856 with a chemist, C. H. G. Williams, synthesizing a blue dye (Figure 1). Williams formed the dye by mixing *N*-amyl quinolinium iodide with *N*-amyl lepidinium iodide in ammonia.ⁱ Because of its hue, *cyanine*, a derivative of the Latin word, *cyanos*, meaning blue, was used to name the structure of the dye.ⁱ Many years later, Wyler, in the 1960's, and Musso, in the 1970's, would discover naturally occurring cyanine dyes.^{ii,iii,iv,v} Betanin, which gives red beets (*Beta vulgaris*) their color, and Musca-aurin, the source of the toadstool fly mushroom (*Amanita muscaria*) fruiting body's orange-red color.⁵

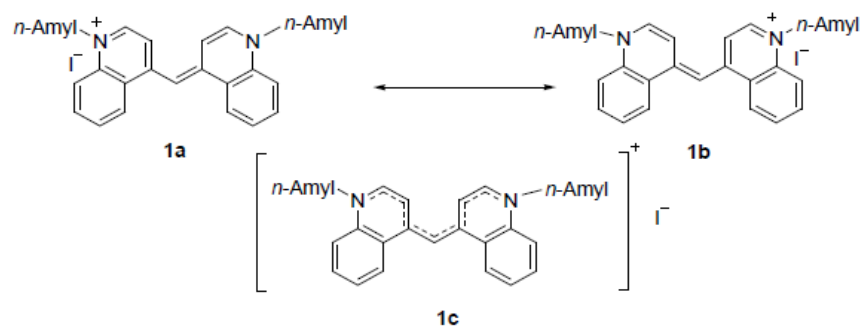


Figure 1. The first synthetic monocyano dye [1].

Structure **1c** shows the delocalized cation created by the additional π electron due to the two heterocyclic aromatic moieties that both act as an electron donor and an electron acceptor.^{vi} These dyes are characterized by a polymethine bridge consisting of $(n+1)$ π electrons, in which n represents the number of sp^2 -hybridized carbons in the methine bridge connecting the two aromatic heterocycle groups (Figure 2).

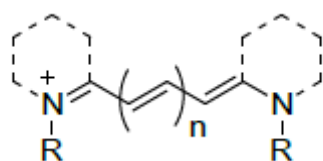


Figure 2. The general structure of cyanine dyes.^{vii}

Mono-, tri-, penta-, and heptacyanine dyes have a methine chain where $n = 0, 1, 2,$ and 3 respectively.^{vii} Variations in the R groups and other substituents attached to the aromatic rings, as well as the number of sp^2 -hybridized carbons in the bridge, affects the absorbance and fluorescence spectra of the molecules. Rigidity greatly increases fluorescence,^{vii} which is a factor for focusing on heptamethine cyanine dyes in this experiment. A vinylene shift, or an increase of $\sim 100\text{nm}$, is seen as n increases and the methine bridge gets longer.^{viii} While the heptamethine cyanine dye is more flexible in solution, when it binds to a biological molecule it

becomes rigid and fluoresces in the visible and NIR region (400-1000nm).^{vii, ix} These absorptive and fluorescent properties give cyanine dyes a wide range of industrial and medical applications.

Polymethine cyanine dyes have increasingly been used since the 1980's when technologies to utilize molecules in the NIR region of the electromagnetic spectrum were created.^{x, xi, xii} Once various technological advancements were achieved, cyanine dyes' chemical and photochemical reactivity could be utilized.^{viii} These attributes have been employed in photographic processes, laser printing, recording media, genomic/proteomic microarrays, and as biological markers for in vivo diagnostic imaging.^{xiii, xiv, xv} The latter is the area of interest and focus of this research.

III. Literature Review

Although more than 150 years have passed since the discovery of the first cyanine dye, the synthesis of these compounds for the purpose of exploiting their photochemical properties for biological imaging agents, and the detection of cancerous tissue, is relatively recent. Within the last decade, the invention of the FLARETM (Fluorescence-Assisted Resection and Exploration) imaging system, by John Frangioni, MD/ PhD, has provided researchers and surgeons with the ability to view normal color video and contrast agents at the same time without impeding their normal vision.^{xvi}

Susan L. Troyan, MD, et al. (2009) tested the FLARETM imaging system's (Figure 3) ability to detect cancerous tissue during oncologic surgery mapping sentinel lymph nodes (SLN) in breast cancer patients.^{xvii} FLARETM uses NIR light to penetrate tissue and excite the molecules of dyes used as imaging agents. This technique offers several benefits to ultrasound or x-ray fluoroscopy, namely that the FLARETM system does not need to be in contact with the

skin, as does ultrasound, and it also does not use damaging ionizing radiation, as does x-ray fluoroscopy.ⁱⁱ Another downfall to the ultrasound and x-ray fluoroscopy techniques is that neither can detect fluorescent markers *in vivo*.^{xviii}

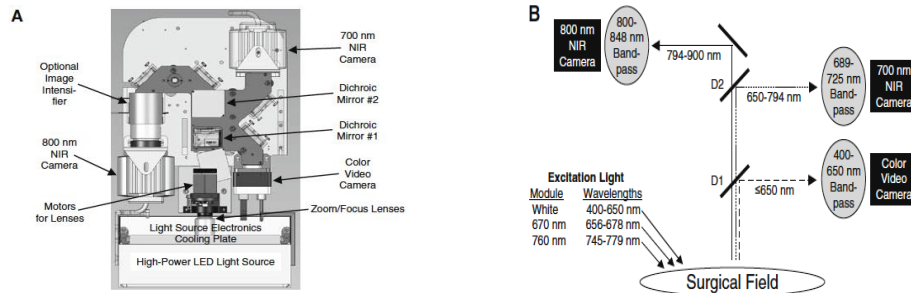


Figure 3: FLARE™ Near-Infrared Fluorescence Imaging System. a Detailed schematic of imaging head. b Optical light paths and filtration for the FLARE™ imaging system having a color video camera, and two independent and simultaneous NIR cameras (700 nm emission and 800 nm emission). D1 = 680 nm dichroic mirror. D2 = 770 nm dichroic mirror.ⁱⁱ

Troyan, MD, et al. used FLARE™ to merge real time video (Figure 4) from three separate cameras (Figure 3B) spanning the visible and NIR spectrum.^{xix} As an imaging agent, Indocyanine Green (ICG) was used in a 1:1 ratio with human serum albumin (HSA). The merging of real-time color video and two grayscale NIR videos, which are then converted to color for image enhancement, proved to be successful in the detection of cancerous tissue.

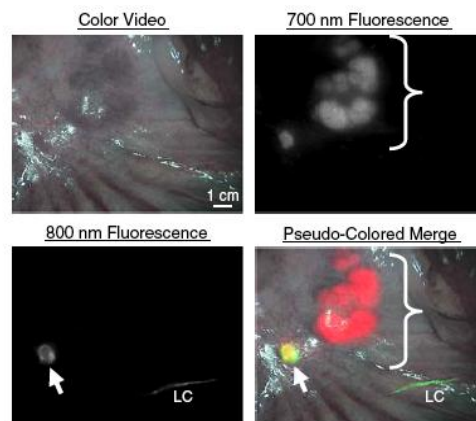


Figure 4: Simultaneous, NIR fluorescent pan-lymph node mapping and sentinel lymph node mapping in swine. All lymph nodes of the mesentery (bracket) fluoresce at 700 nm (pseudo-colored red) after a single intravenous injection of 1 mg/kg of methylene blue. SLN (arrow) fluorescing at 800 nm (pseudo-colored green) is identified after intraparenchymal injection of 10 μM of ICG:HSA into the colon wall, and appears yellow. The lymphatic channel (LC) feeding the SLN appears green. All camera exposure times were 67 msec. Data are representative of n = 5 pigs.ⁱⁱ

For more than thirty years, ICG (Figure 5) has been used for the imaging of the retina and chorion.^{xx,xxi} In a research paper by T. Desmettre, MD/PhD, et al. (2000), properties of ICG, namely molecular weight, metabolic features, and photochemical properties, were exploited for the imaging of retina and chorion vasculature.^{xxii} ICG, a heptamethine cyanine dye, is amphiphilic, so it can interact with lipophilic molecules, while still being polar enough to dissolve in aqueous solution.^{xxiii,xxiv}

Pharmacokinetics showed ICG to be relatively safe, having a plasmatic half-life of 2-4 minutes, and a rapid elimination by liver cells.^{xxv,xxvi,xxvii,xxviii} However, while ICG could be successfully injected into ocular tissues and remain there for approximately 12 minutes due to

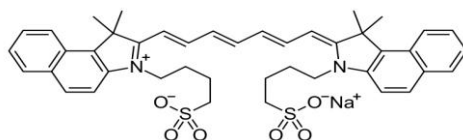


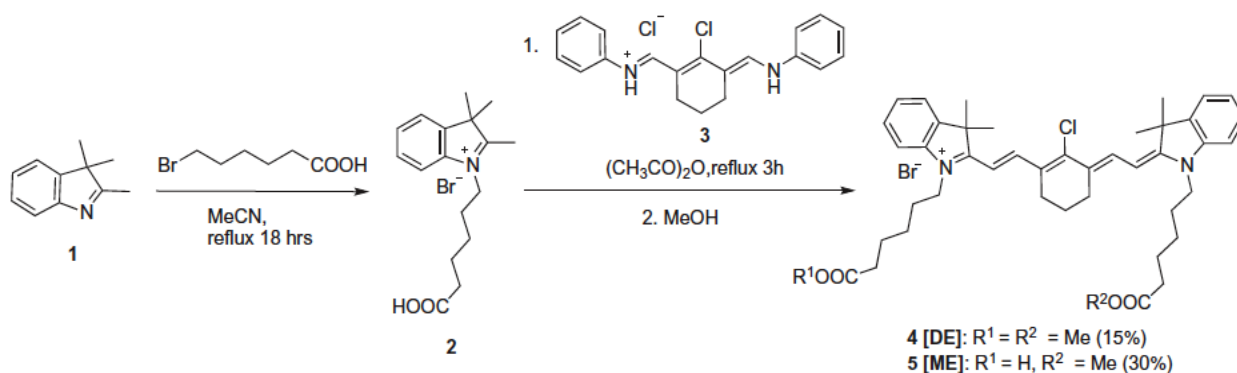
Figure 5: Structure of Indocyanine Green dye.

its affinity for plasma proteins and lipoproteins,^{xxix,xxx,xxxi,xxxii} its binding specificity is not limited to the vasculature of the eye. Specificity of ICG can prove to be an issue partially because of its amphiphilic properties. However, the synthesis techniques used (Scheme 1) in the production of other heptamethine cyanine dyes by the Maged Henary Lab, at Georgia State University, works to solve such problems.

Selectivity is always a desirable characteristic for an imaging probe to have, essentially dictating how effective the probe is at functioning in the manner for which it was intended. After the successful synthesis and purification of several heptamethine cyanine dyes, using a facile one

pot method^{xxxiii}, Maged Henary, PhD, et. al (2012), used the trypan blue assay^{xxxiv} to confirm that two of the synthesized compounds, a monoester (**4**. ME) and diester (**5**. DE) dye, were indeed highly specific and cytotoxic to cancer cells, while leaving viable cells unharmed. The tests were performed in vitro, using human cervical (HeLa) and prostate (PC-3) cancer cells for the experimental group, and primary human dermal fibroblast (HDF) viable cells as the control.

Tests were also conducted to determine the dyes' effects on proliferation in both cancerous and healthy cell lines. Results for both the ME and DE compounds indicated that at very low concentrations proliferation of cancerous cells were halted, while it took as much as a 10-fold increase in concentration to terminate the proliferation of healthy cells. This huge difference in concentration constitutes a wide therapeutic window in which to target tumors.



Scheme 1. Synthetic route for the preparation of heptamethine cyanine dyes 4–5.

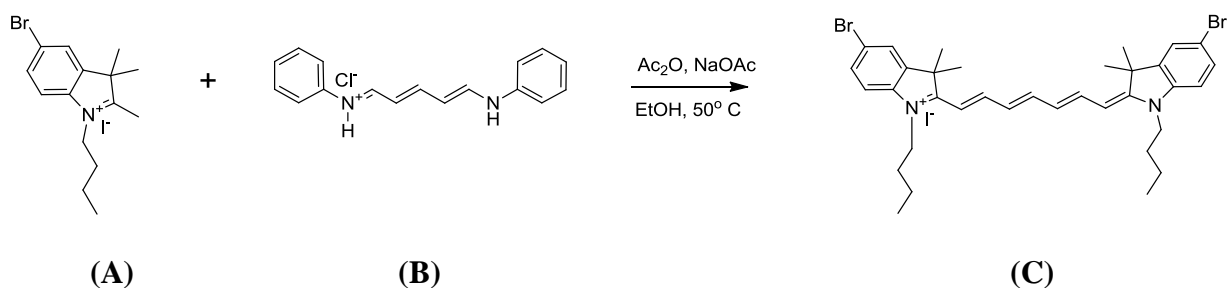
With such interesting data, there has been an increased interest in NIR polymethine cyanine dyes as imaging agents given the advancements in imaging detection technologies. The properties of these dyes that, with the help of new technologies, give researchers and physicians the ability to see real-time images in both the visible and near-infrared spectra (Desmetre, et al. 2000; Henary, et. al 2012; Troyan, et al. 2009). Earlier dyes' lack of specificity for a target

influenced the research of dyes that had this quality. With the discovery of cyanine dyes, some possessing high levels of specificity, NIR cyanine dyes are now an important area of focus for diagnostic imaging for guided surgery, cancer detection and research, and fluorescent probes. With two NIR cyanine dyes also being selectively cytotoxic to cancer cells, while leaving the viable cells in a state of proliferation, these compounds may serve a dual purpose in the fight against cancer; one of detector and destroyer.

IV. Methods

Heptamethine Cyanine Dye

To prepare the final product (Equation 1C) a 2:1 molar ratio of starting reagents **A**:**B** was used. In a 250 mL round bottom flask, reagent **A** (1.0 g, 2.4 mmol) was combined with 10 mL ethanol (EtOH), 1 mL acetic anhydride (Ac₂O), and 1.2 molar equivalents of sodium acetate (NaOAc). A magnetic stir bar was added to the flask, and the mixture was placed in oil on a hot plate (50°C, 30 min). A condenser was used to limit evaporation. Next reagent **B** (0.3 g, 1.1 mmol) was added to the solution, and the reaction was left to stir overnight (50°C, 24 h). Ethyl ether was used to precipitate product **C** from the solution, and it was isolated using vacuum filtration.



Equation 1: Synthesis of heptamethine cyanine dye.

Proton NMR (H^1 NMR) was done to determine purity. Impurities remained, and further purification via re-crystallization was performed by dissolving the product in methanol (MeOH), then using ethyl ether to precipitate the crude solid. A new H^1 NMR spectrum was obtained, but impurities were still present.

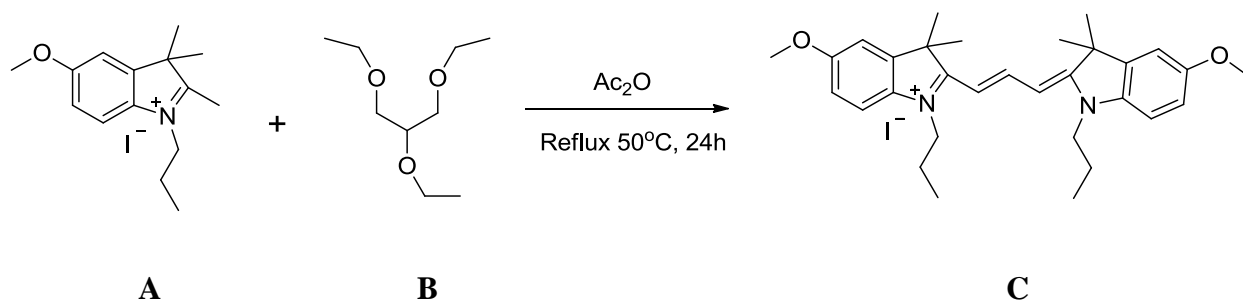
A Thin Layer Chromatography (TLC) test indicated that dichloromethane (DCM) had no effect on product C, so this solvent was used to remove impurities. Flash Column Chromatograph was used to purify the product, starting with 100 mL batches of DCM, to remove polar impurities. After several rinses, 1 mL doses of MeOH were added to the DCM until there was a final ratio of 100:1 DCM:MeOH. When the ratio of the solvent system was 25:1, pure product began to elute. Multiple fractions were collected, roto-vapped, and dried.

New H^1 NMR spectra were taken, one for fractions 1-8, and one for fractions 9-14. Both spectra indicated pure product. Finally, a C^{13} NMR spectrum was obtained, further indicating the purity of the product (118 mg, 0.152 mmol).

Trimethine Cyanine Dye

In a 250 mL round bottom flask the indolium iodide salt (0.271 g, 0.754 mmol) (Equation **2A**) was added with the linker reagent (0.65 mL) (Equation **2B**) in Ac_2O (5 mL) and refluxed (50°C, 24 h). The reaction was monitored using UV Vis until complete. Diethyl ether was added to the round bottom flask (in excess) to facilitate precipitation of the product (Equation **2C**). The

flask was placed in a refrigerator (4°C, 24 h) and recrystallized (MeOH, ether). Further



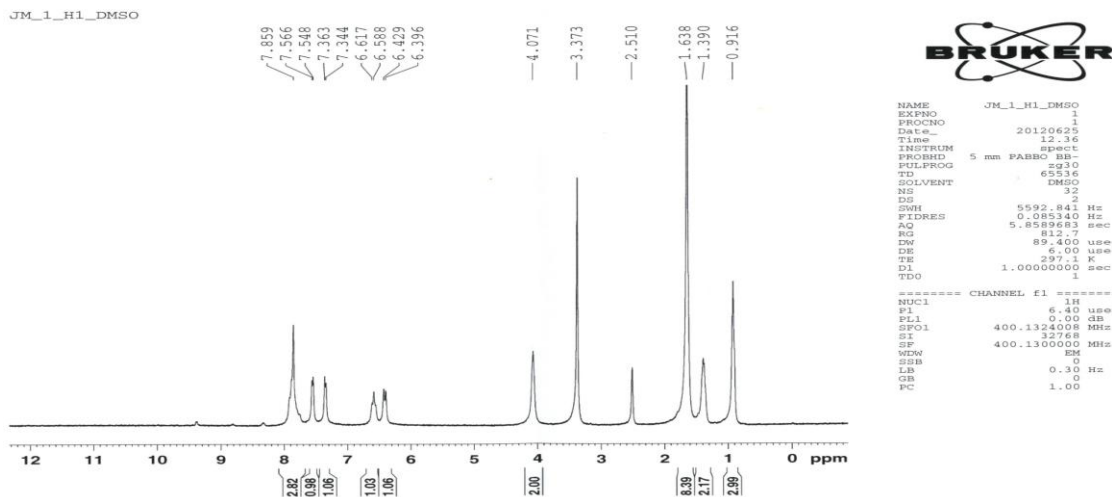
Equation 2: Synthesis of trimethine cyanine dye

purification was accomplished using chromatotron centrifugal thin layer chromatography (DCM:MeOH). The product was condensed on the rotovap and allowed to dry in a vacuum desiccator for a week to yield final product (83.2 mg, 0.139 mmol).

V. Results/Data Analysis

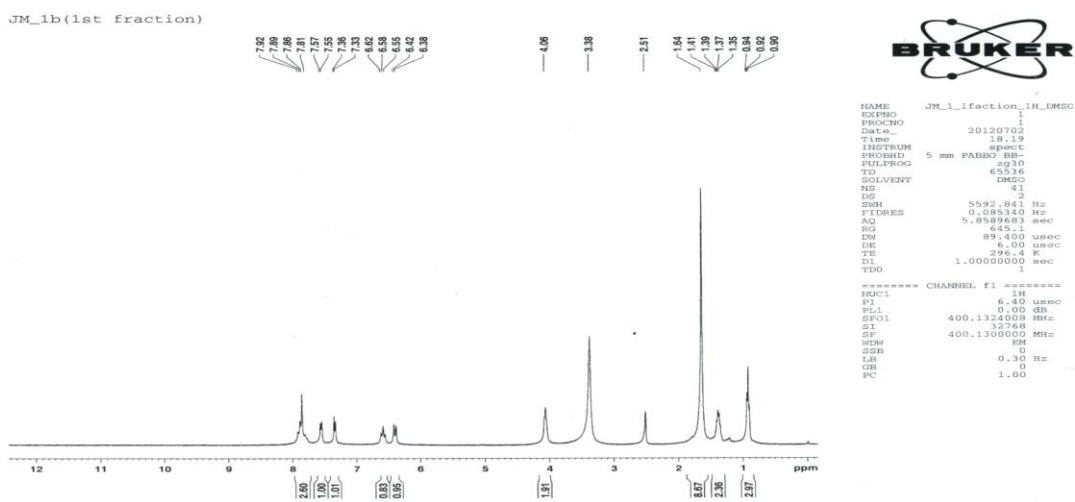
Heptamethine Cyanine Dye

Initial analysis of the proton nuclear magnetic resonance (H^1 NMR) spectrum for the final dye (Scheme 2C) showed four small impurities between ~ 8 -12 ppm. Re-crystallization was done in an attempt to remove these impurities. The sample was dissolved in methanol (MeOH), and then precipitated using diethyl ether. This was performed twice to optimize chances of purification. A second H^1 NMR was run on the newly re-crystallized compound (Spectrum 1), and while analysis indicated the small impurity peak located at ~ 12 ppm was removed, three small ancillary peaks remained at ~ 8 -9.5 ppm. Failure to remove all impurities via re-crystallization indicated a different purification technique was needed.



Spectrum 1: ^1H NMR taken after additional re-crystallization in MeOH and diethyl ether. A small impurity at ~ 12 ppm was removed, but three additional impurity peaks remained between ~ 8 -9.5 ppm.

Flash column chromatography was used to purify the sample, and a final ^1H NMR spectrum was taken (Spectrum 2). The new spectrum showed a clean baseline where the previous impurities were located, indicating that column chromatography was successful in purifying the sample. Additionally, after disregarding two peaks (2.510, 3.373 ppm) associated with DMSO, the solvent used to dissolve the dye, the ^1H NMR closely resembled the estimated spectrum (Figure 6) obtained using ChemDraw software.



Spectrum 2: Final ^1H NMR taken for synthesized heptamethine cyanine dye indicating purity.

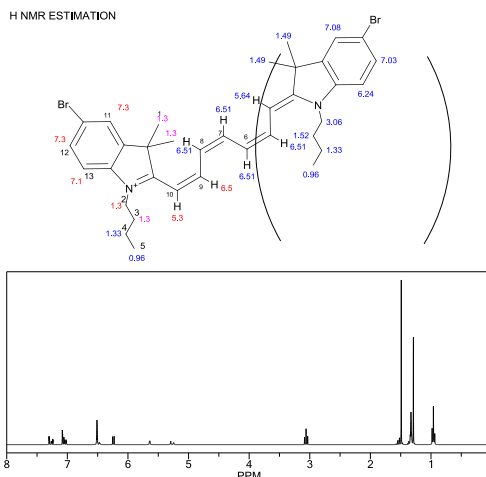
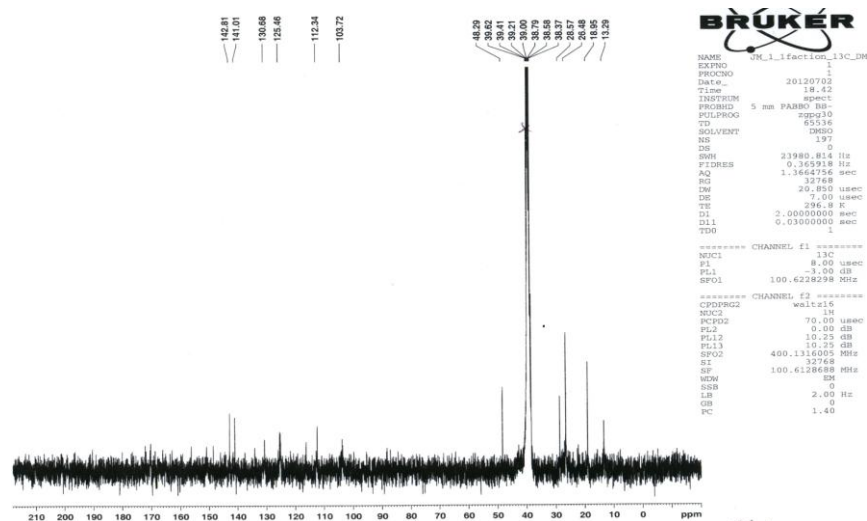


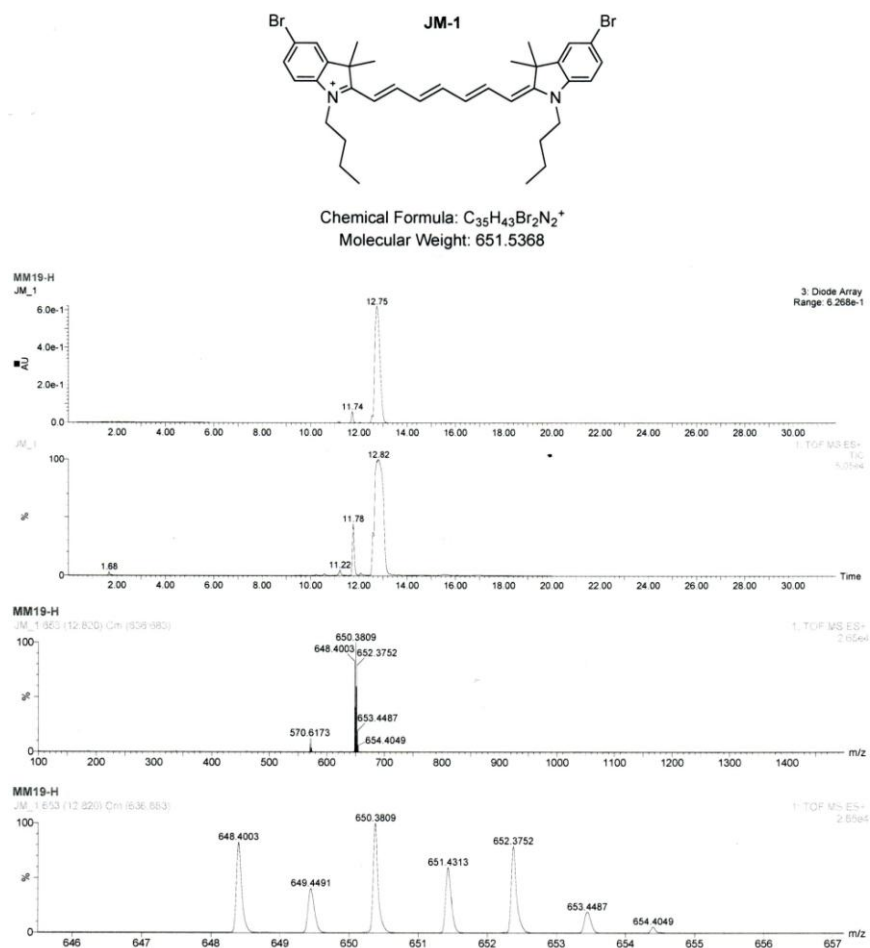
Figure 6: Estimated ^1H NMR predicted by ChemDraw software. In the drawing of the structure above the spectrum, approximate locations (ppm) are given for the 13 different hydrogen atoms in the compound.

With all hydrogen atoms for the expected dye accounted for, next a carbon-thirteen nuclear magnetic resonance (C^{13} NMR) was taken to further verify that the intended dye was actually produced. The first C^{13} NMR spectrum, using 197 scans, was missing four quaternary carbons, which was expected on a spectrum with a low number of scans. A second C^{13} NMR spectrum was taken using 3165 scans (Spectrum 3), identifying two of the four quaternary carbons, while two were shielded by the baseline.



Spectrum 3: Final C^{13} NMR of synthesized heptamethine dye.

Finally, a sample of the compound was tested for absorbance, and injected into a column for liquid chromatography and mass spectrum analysis (LCMS). The absorbance spectrum indicated the compound absorbed light at 754 nm, precisely in the anticipated near-infrared region of the electromagnetic spectrum. The data for the LCMS (Spectrum 4) further reflected positive results. An intense peak, coming off of the LC column at 12.75 minutes, corresponds to a 98% pure compound. Furthermore, with the exact mass of the heptamethine cyanine dye (plus one hydrogen atom) being 650.1788 g/mol, the most intense peak on the MS analysis, 650.3809 g/mol, is almost identical. Anticipated splitting patterns for the compound were also verified.



Spectrum 4: Liquid Chromatography and Mass Spectrum Analysis of the heptamethine cyanine dye. Liquid Chromatography indicated a pure compound, indicated by one major peak of absorbance, while Mass Spectrum Analysis verified the presence of the synthesized compound by molecular weight and anticipated splitting patterns.

After the compound was purified and characterized, it was sent for *in vivo* testing at the Hak Soo Choi and John V. Frangioni Laboratories at Beth Israel Deaconess Medical Center, Harvard University. Between 2-25 nmol of dye, in a 30% FBS saline solution, was injected in the penile vein of CD-1 (n=1) mice and tracked. Using the FLARE imaging system, surgeons superimposed the video from a color camera, filming in the visual spectrum of light, and a second camera, recording in the NIR region. The results of the test showed binding in the vasculature of the brain, however, the dye did not cross the blood brain barrier (Figure 7).

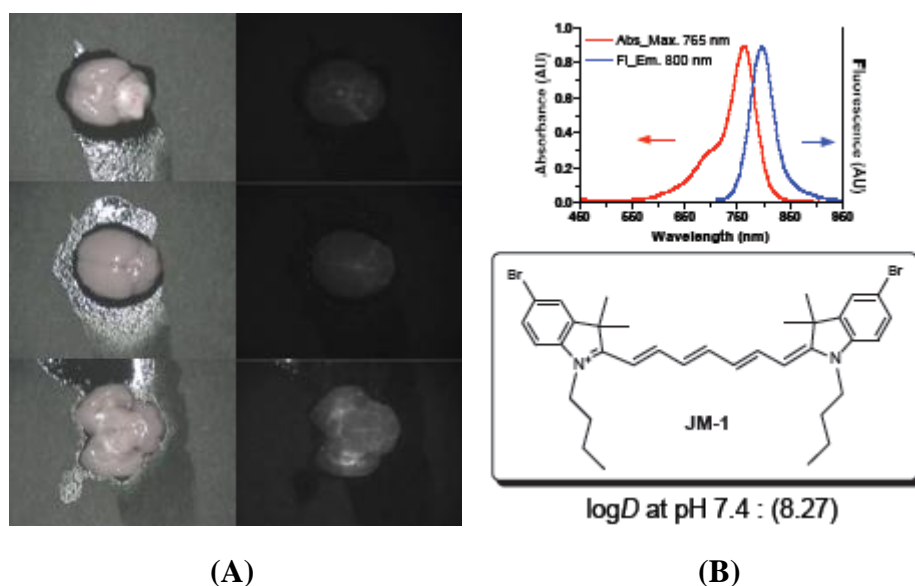


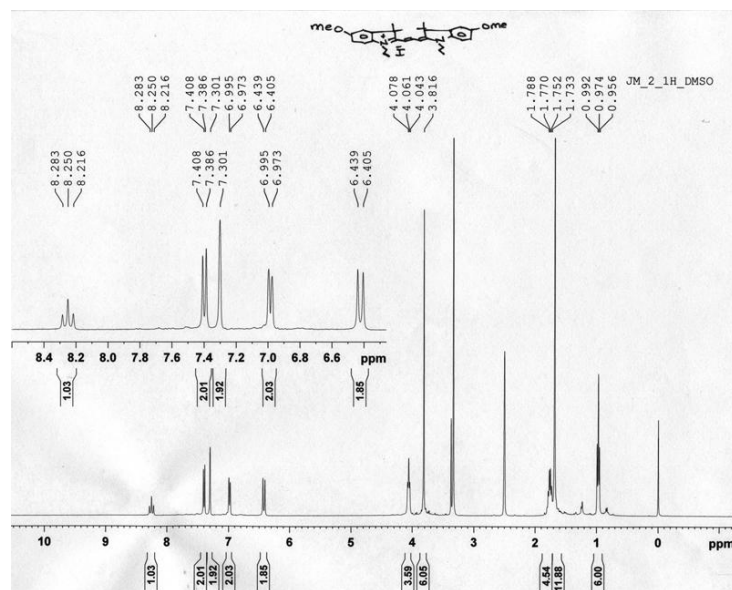
Figure 7: (A) Three views of a mouse brain (bottom, top, cross section) following injection of the heptamethine dye (B bottom) through the penile vein. (B) Absorption and fluorescence spectra (top) of the dye (structure bottom).

Trimethine Cyanine Dye

After several rounds of recrystallization trying several solvent systems (hexanes, MeOH:ether, MeOH:hexanes:ether) the product continued to have an oily state. Using chromatotron centrifugal thin layer chromatography, the product was further purified using DCM:MeOH. The DCM removed the initial impurities, while the MeOH pushed the polar dye down the silica plate to be collected. Fractions containing the product were combined and

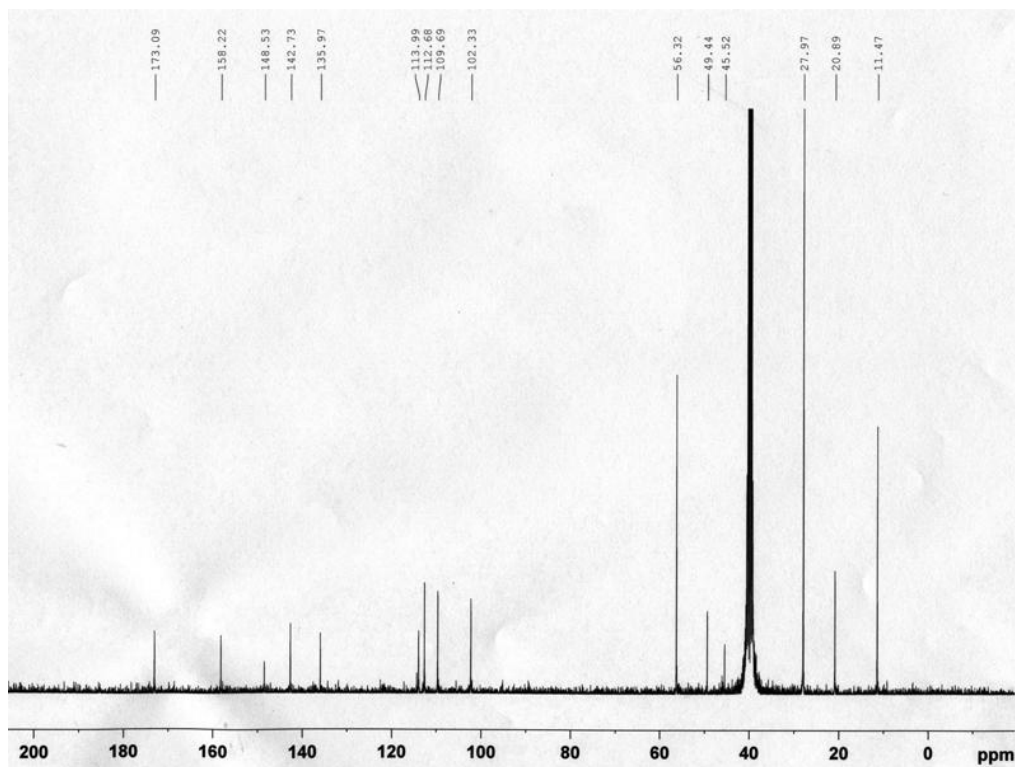
concentrated using rotovap, and the resulting crystals were collected and submitted for H^1 NMR analysis. The presence of a solvent impurity peak resulting in leaving the dye in a vacuum desiccator (2 wk) to ensure the product was completely dry.

A supplemental H^1 NMR (Spectrum 5) was taken and indicated the product had been purified. The spectrum indicated the presence of 41 hydrogen atoms, which correlates to the correct number of hydrogen atoms in the molecule. Peaks between 3.5-4 ppm represent six hydrogen atoms, three attached to each methoxy group on carbon 5 of the benzene rings. Eight hydrogen atoms between 6.5-8 ppm show the presence of the four hydrogen atoms on each benzene ring (C4-C7), while 12 hydrogen atoms between 1-2 ppm represent the two dimethyl groups on C2 of the heterocycles. The fourteen hydrogen atoms on the n-propyl substituents are shown by six atoms (1 ppm), 4.54 atoms (1.8 ppm), and 3.5 atoms (4.1 ppm). The latter 3.5 atoms represent those closer to the positive nitrogen atom of the heterocycle, which causes them to appear further downfield. The placement of these atoms indicates the desired structure was achieved.

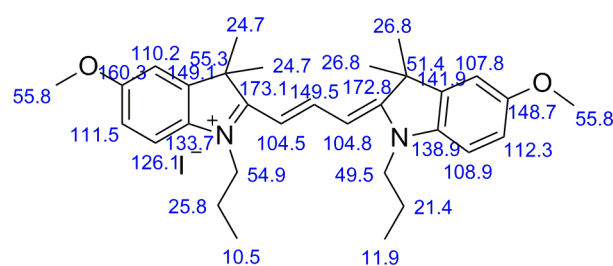


Spectrum 5: H^1 NMR of trimethyl cyanine dye

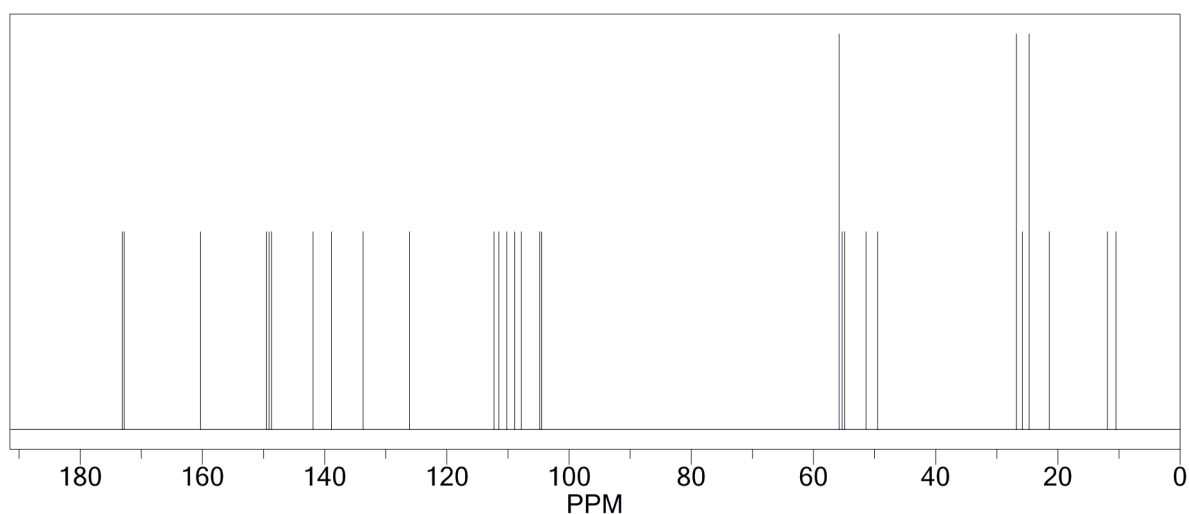
Further analysis of a C^{13} NMR (Spectrum 6) showed the product was formed. The spectrum was compared with a proposed spectrum using ChemDraw software (Spectrum 6), and the two were very similar. The aliphatic carbons were located between 10-60 ppm. The largest peak at 27.97 ppm indicates the two dimethyl carbon atoms attached to the heterocycle. The peak at 56.32 indicates the carbon atoms attached to the oxygen on the methoxy group, while the third largest aliphatic peak at 11.47 indicates the third carbon atoms on the tip of the propyl substituent. The peaks at 20.89 and 49.44 ppm represent the other two carbons in the n-propyl chain, with the carbon atom closest to the nitrogen of the heterocycle appearing farthest down field. The other peaks (100-114 ppm) indicate the aromatic carbons (electron rich), while the remaining peaks (135-159 ppm) represent the carbons in the methine bridge (electron poor).



Spectrum 6: C NMR of trimethyl cyanine dye

ChemNMR ^{13}C Estimation

Estimation quality is indicated by color: **good**, **medium**, **rough**



Spectrum 7: Projected C NMR of trimethine cyanine dye from ChemDraw software

VI. Conclusion

For this experiment, a multi-step synthetic approach was used to synthesize a NIR heptamethine and trimethine cyanine dye. Purification through re-crystallization was not effective in removing all impurities found using ^1H NMR spectrum analysis for either dye. A pure product was ultimately obtained for the heptamethine dye by means of flash column chromatography, with a solvent system of DCM:MeOH in a 25:1 ratio. The trimethine dye was purified using chromatotron centrifugal thin layer chromatography with a similar DCM:MeOH ratio. With a pure heptamethine cyanine dye product isolated, characterized, and purified, a sample was sent

to the Choi and Frangioni Laboratories at Harvard University. Because of the photochemical properties of this molecule, in vivo testing was performed on a rat model, and the effectiveness of utilizing this dye as a biological imaging agent was investigated. The results of the experiment showed interesting activity within the vasculature of the brain. Further studies will be performed to ascertain what the possible diagnostic and/or medical applications of this dye may be.

The pure trimethine cyanine dye was sent to the George Zheng Lab at Georgia State University. The Zheng Lab studies the effects of protein arginine methyltransferase (PRMT) activity, and the role that methylation of various molecules plays a role in cancer formation, cardiac disease, and pulmonary disorders. Further research will be done using the trimethine cyanine dye as a mean to inhibit this methylation of the amino acid arginine, and thus prohibit formation of various cancers.

References

-
- ⁱ Tyutyulkov N, Fabian J, Mehlhorn A, Dietz F, Tadjer A (1991) *Polymethine Dyes: Structure and Properties*; St. Kliment Ohridski University Press: Sofia, Bulgaria
- ⁱⁱ Wyler, H. *Chem Unserer Zeit* **1969**, 3,111.
- ⁱⁱⁱ Wyler, H. *Chem Unserer Zeit* **1969**, 3,146.
- ^{iv} Musso, H. *Tetrahedron* **1979**, 35, 2843.
- ^v Reichardt, C. *J Phys Org Chem* **1995**, 8, 761.
- ^{vi} Mason, C. J., Georgia State University, 2001.
- ^{vii} Mojzych, M.; Henary, M. In *Topics in Heterocyclic*; Streckowski, Ed.; Springer: Berlin, 2008; Vol. 14, p 1. Verlag, Heidelberg.
- ^{viii} Fernando, N. T., Georgia State University, 2011.
- ^{ix} Sturmer DM (1977) In: Weissberger A, Taylor EC (eds) *The chemistry of heteroaromatic compounds*, vol 30. Wiley, New York
- ^x Baars, M.; Patonay, G., Ultrasensitive detection of closely related angiotensin I peptides using capillary electrophoresis with near-infrared laser-induced fluorescence detection. *Anal Chem* **1999**, 71, (3), 667-71.
- ^{xi} Tarazi, L. G., A.; Patonay, G.; Streckowski, L., Spectral characterization of a novel near-infrared cyanine dye: a study of its complexation with metal ions. *Talanta* **1998**, 46, (6).
- ^{xii} Legendre, B. L.; Moberg, D. L.; Williams, D. C.; Soper, S. A., Ultrasensitive near-infrared laser-induced fluorescence detection in capillary electrophoresis using a diode laser and avalanche photodiode. *Journal of Chromatography A* **1997**, 779, (1-2), 185-194.
- ^{xiii} Gragg, J. L., Georgia State University, 2010.
- ^{xiv} Shi, C.; Zhang, C.; Su, Y.; Cheng, T. *The Lancet* 2011, 11, 815.
- ^{xv} Mishra, A., Behera, R. K., Behera, P. K., Mishra, B. K., and Behera, G. B. (2000) Cyanines during the 1990s: A Review. *Chem. Rev.* 100, 1973–2012.
- ^{xvi} Nakayama A, del Monte F, Hajjar RJ, Frangioni JV. Functional near-infrared fluorescence imaging for cardiac surgery and targeted gene therapy. *Mol Imaging*. 2002;1:365–77.

^{xvii} Troyan, M.D., S. L., Kianzad, PhD, V., Gibbs-Strauss, PhD, S. L., Gioux, MEng, S., Matsui, M.D., PhD, A., Oketokoun, MEng, R., & Ngo, PhD, L. (2009). The FLARE Intraoperative Near-Infrared Fluorescence Imaging System: A First-in-Human Clinical Trail in Breast Cancer Sentinel Lymph Node Mapping [Electronic version]. *Annals of Surgical Oncology*, *16*, 2943-2952. doi:10.1245/s10434-009-0594-2

^{xviii} Frangioni JV. New technologies for human cancer imaging. *J Clin Oncol*. 2008;*26*:4012–21.

^{xix} Gioux S, Kianzad V, Ciocan R, Gupta S, Oketokoun R, Frangioni JV. High power, computer-controlled, LED-based light sources for fluorescence imaging and image-guided surgery. *Mol Imaging*. 2009 (in press).

^{xx} Benson RC, Kues HA: Fluorescence properties of indocyanine green as related to angiography. *Phys Med Biol* 23:159–63, 1978

^{xxi} Flower RW: Evolution of indocyanine green dye choroidal angiography. *Optical Engineering* 34:727–36, 1995

^{xxii} Landsman ML, Kwant G, Mook GA, Zijlstra WG: Light-absorbing properties, stability, and spectral stabilization of indocyanine green. *J Appl Physiol* 40:575–83, 1976

^{xxiii} Devoisselle JM, Mordon S, Soulie S, Desmettre T, Maillols H: Fluorescence properties of indocyanin green/part 1: in vitro study with micelles and liposomes, in Lakowicz JR, Thompson JB (eds): *Advances in Fluorescence Sensing Technology III*; 1997. Bellingham, CA, USA, SPIE, 1997, pp. 530–37

^{xxiv} Dobashi A: 3D modelization of the ICG molecule. <http://www.ps.toyaku.ac.jp/~dobashi/english/>, 1999

^{xxv} Cherrick GR, Stein SW, Leevy CM, Davidson CS: Indocyanine green: observations on its physical properties, plasma decay and hepatic extraction. *J Clin Invest* 39:592–600, 1960

^{xxvi} Flock ST, Jacques SL: Thermal damage of blood vessels in a rat skin flap window chamber using ICG and a pulsed alexandrite laser: a feasibility study. *Laser Med Sci* 8:185–96, 1993

^{xxvii} Hollins B, Noe B, Henderson JM: Fluorometric determination of indocyanine green in plasma. *Clin Chem* 33:765–8, 1987

^{xxviii} McEvoy G: AHFS Drug Information. in American Society of Hospital Pharmacy, 1990.

^{xxix} Auer C, Bernasconi O, Herbort CP: Indocyanine green angiography features in toxoplasmic retinochoroiditis. *Retina* 19:22–9, 1999

^{xxx} Baker KJ: Binding of sulfobromophthalein (BSP) sodium and indocyanine green (ICG) by plasma alpha-1 lipoproteins. *Proc Soc Exp Biol Med* 122:957–63, 1966

^{xxxi} Auer C, Herbort CP: Indocyanine green angiographic features in posterior scleritis. *Am J Ophthalmol* 126:471–6, 1998

^{xxxii} Herbort CP, LeHoang P, Guex-Crosier Y: Schematic interpretation of indocyanine green angiography in posterior uveitis using a standard angiographic protocol. *Ophthalmology* 105:432–40, 1998

^{xxxiii} Henary, M.; Pannu, V.; Owens, E. A.; Aneja, R.; *Bioorganic & Medicinal Chemistry Letters*. 2012, 22, 1242.

^{xxxiv} Zhou, J.; Liu, M.; Luthra, R.; Jones, J.; Aneja, R.; Chandra, R.; Tekmal, R. R.; Joshi, H. C. *Cancer Chemother. Pharmacol.* 2005, 55, 461.